ELEKTRIKA
Journal of Electrical Engineering

Inductive Helical Stent for Wireless Revascularization: Finite Element Analysis

Yong Xian Ang and **Mohamed Sultan Mohamed Ali**[*]

School of Electrical Engineering, Universiti Teknologi Malaysia, 81310 Johor Bahru, Johor, Malaysia.
[*]Corresponding author: sultan_ali@fke.utm.my, Tel: +607-5557165, Fax: +607-5566272

Abstract: This paper reports simulation of a shape-memory-alloy (SMA) nitinol type active stent for wireless revascularization. The device comprises an inductive helical stent as an inductive component and a capacitive pressure sensor as a capacitive component. When the stent is coupled to an external coil with a radiofrequency (RF) signal, the stent can be expanded wirelessly by matching the signal with the device resonant frequency. By this approach, restenosis in a stented vessel can be potentially eliminated without a repeat stenting procedure. However, the calculation of important parameters is difficult using the conventional analytical method due to the unconventional structure of the helical stent which can be considered an irregular solenoid. In this work, finite element analysis (FEA) was performed using ANSYS HFSS to simulate the inductance, quality factor, and series resistance of the device at the initial crimped state and expanded state as a function of frequency.

1. INTRODUCTION

Ischemic heart disease (IHD) is a major cause of mortality worldwide, leading to 16,325 deaths in Malaysia which is 0.18% out of 8.9 million global cases in 2019 [1-2]. Ischemic is a term that refers to the condition of inadequate blood supply to blood vessels. The primary pathological process that causes IHD is the progressive narrowing of a blood vessel (stenosis) due to the lipid deposition and plaque proliferation on the artery walls. The build-up of plaque causes the thickening and hardening of artery known as atherosclerosis. IHD results in coronary syndromes such as ischemic chest pain (angina pectoris) or heart attack (myocardial infarction).

One of the treatments for IDH is called percutaneous transluminal angioplasty (PTA). PTA is a minimally invasive endovascular procedure performed to resolve atherosclerotic lesions. During an angioplasty, a balloon equipped at the tip of a catheter is inflated to expand the narrowed arteries for revascularization. Yet, the mechanical radial force applied on the target vessel wall initiates an inflammatory response known as re-narrowing or restenosis, which lasts for a long time after the angioplasty [3]. Therefore, an implantable tiny tube known as a stent has been introduced and deployed after balloon angioplasty to physically dilate and scaffold target vessels.

Although the introduction of the balloon-expandable bare-metal stents has improved PTA by effective revascularization, the restenosis rate remains high as 30% due to progressive intimal hyperplasia [4]. Intimal hyperplasia is the proliferation and thickening of smooth muscle cells which occur at the intimal layer inside an implanted stent. This undesired consequence of PTA is also known as in-stent restenosis (ISR). To address the higher rate of ISR, drug-eluting types of stents are developed by adding a layer of anti-proliferative agent on the bare-metal stents. The embedded drugs within anti-proliferative agents function to mitigate the in-stent overgrowth of endothelial tissues.

Yet, the use of a drug-eluting approach by inducing the delay of the endothelial healing process may lead to blood clot formation at the stented vessel. This issue is known as in-stent thrombosis and is a life-threatening acute complication that causes mortality [5-7]. Repeat stenting procedure is one of the treatments to resolve ISR which will occur at a substantial rate. Drug-eluting stents are used to overlap previously implanted stents for subsequent revascularization [8-9]. Compared to the repeat stenting approach, newer types of stents such as biodegradable polymer types and bioabsorbable metallic types of stents have been developed to provide stent post-removal mechanism as an alternative approach to resolving ISR. However, these newer stents are having issues of material instability and long-term effect [10-13].

In efforts to overcome the limitation of the aforementioned stent types to eliminate ISR, novel stents have been developed. One of them is an electrothermally-activated stent that uses a hyperthermia approach to inhibit ISR. This type of stents makes use of a micro-electro-mechanical system (MEMS)-based technique to realize the controllable wireless stent heating feature up to ~45 °C as a ballpark for cell tissue heat tolerance [14-17]. The

MEMS-based active stent comprises an inductor-capacitor (LC) resonant circuit configuration for its functionality [18-21]. Apart from wirelessly driven resonant heating in the inductive stent, the capacitive component can be replaced with a capacitive pressure sensor for wireless blood pressure monitoring capability. This would provide a real-time approximate blood pressure reading to detect ISR prior to angiography or ultrasound diagnosis performed by a cardiovascular radiologist.

The inductive component is a helical type conductive stent that functions as an inductive antenna to be coupled with an external coil for wireless heating or wireless monitoring [22-23]. However, conventional stainless-steel type helical stents may not resolve the re-narrowing issue when hyperthermia treatment is unable to inhibit ISR. Hence, an SMA-type active stent is developed to overcome the limitation. Nitinol, which is one type of SMA material, enables a crimped active stent to be expanded wirelessly by wireless heating when ISR emerges [24]. This approach potentially eliminates the necessity for subsequent revascularization by repeat stenting procedure.

The MEMS-based SMA nitinol-type active stent used to realize the wireless revascularization feature is an inductive helical stent. The unconventional helical shape with serpentine stent struts functions as a scaffold to provide more surface coverage to the target vessel. In addition, this shape and structure make the critical values i.e., inductance, quality factor, and series resistance difficult to be calculated using the conventional analytical method. Hence, FEA is used as an alternative approach to obtain the values which are critical in this RF device application. This paper reports a simulation of the inductance value, quality factor, and series resistance of the aforementioned inductive helical stent via FEA at the initial crimped state and expanded state as a function of frequency. The simulation would help to obtain a better stent design in terms of shape and geometry before the fabrication process, saving extra possible costs.

2. WORKING PRINCIPLE AND DESIGN

Nitinol is a smart material that manifests a shape memory effect. It is commonly used in biomedical implantable devices due to its biocompatibility. It is characterized by a "soft" martensitic phase and a "rigid" austenitic phase, which exist at low and high temperatures, respectively. The nitinol memorizes a pre-determined shape at the austenitic phase. The transformation between the two phases is applied for the procedure between crimping and deployment of the aforementioned SMA nitinol-type active stent.

During PTA, balloon angioplasty is usually performed prior to the stenting procedure. The active stent at the martensitic phase can be crimped mechanically by radial compressive force. The pre-crimped stent is mounted on a catheter to be inserted and delivered to the target vessel via transradial or transfemoral access. The stent will be deployed subsequently to restore the blood flow. When this MEMS-based active stent is equipped with a capacitive pressure sensor, it can wirelessly detect ISR occurrence by estimating the changes in blood pressure. An external coil can be coupled to the active stent for blood pressure reading.

When there is a pressure reading indicating the need for revascularization due to the ISR occurrence, an RF signal that matches the resonant frequency of the active stent can be used to induce resonant heating. The heat-induced will transform the stent back to the austenitic phase and restore the pre-determined stent shape. Thus, the active stent can be wirelessly re-expanded to treat ISR, potentially eliminating the need for repeat stenting. Figure 1 shows the device design comprises an inductive helical stent (inductive component) and a capacitive pressure sensor (capacitive component) to form an LC resonant circuit.
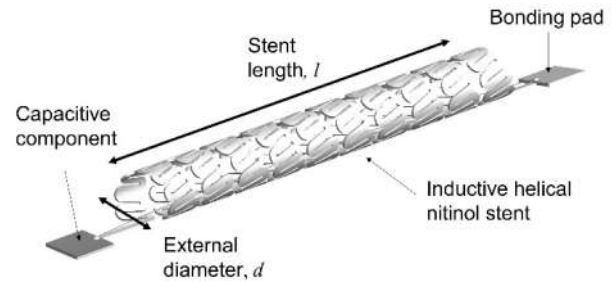

Figure 1. Inductive wireless stent design.

The active stent has a resonant frequency,

$$f_R = \frac{1}{2\pi\sqrt{LC}} \tag{1}$$

where L is the inductance of the inductive helical stent and C is the capacitance of the capacitive component. The inductive helical stent is connected in series with the capacitive component to form a closed-loop resonant circuit. Using Equation (1), an active stent with a desired resonant frequency can be established by choosing an appropriate capacitance value for the capacitive component given the inductance values of the inductive helical stent are known.

In this work, a design of an inductive helical stent with a serpentine strut profile is used to increase the surface coverage on the artery wall. However, the inductance of the stent with serpentine strut profile cannot be accurately determined from a conventional solenoid inductance equation. The inductance of a solenoid equation is used for approximation as follows.

$$L = \frac{\mu_r\mu_0 N^2\pi d^2}{4l} \tag{2}$$

where μ_0 is the magnetic permeability of free space, N is the number of turns, d is the diameter of the inductive helical stent, and l is the length of the inductive helical stent. The diameter of the inductive helical stent changes when it is expanded. Thus, the stent at initial crimped and expanded states has different inductance values.

In general, the stent inductance is related to the stent geometrical structure and the surrounding medium with relative magnetic permeability, μ_r. To assess the

performance of wireless power transfer efficiency, the quality factor, Q is a parameter to consider. Q is the ratio of inductive reactance X_L to the resistance R as follows.

$$Q = \frac{X_L}{R} \qquad (3)$$

$$X_L = 2\pi f L \qquad (4)$$

The series resistance of the stent can be calculated as

$$R = \rho \frac{L_s}{A} \qquad (5)$$

where ρ is the electrical resistivity of nitinol depends on whether austenitic or martensitic phases, Ls is the total length of continuous stent wire, and A is the cross-sectional area of the stent wire.

3. FINITE ELEMENT ANALYSIS

Finite element analysis was performed to obtain the values of L, Q, and R of the inductive helical stent using ANSYS HFSS. The 3D model of the stent was designed in SolidWorks and imported to HFSS. Figure 2 shows the setup of the stent in HFSS. The distal and proximal ends of the stent are connected with lumped ports for excitation. The inductance value is related to the stent geometry and the medium surrounding the stent, which is air in this simulation. The air domain has a magnetic permeability value which is close to vacuum. Table 1 shows the parameter values of nitinol to be set in HFSS material library. The bulk conductivity is the reciprocal of the electrical resistivity depending on the crystal structure: either martensite or austenite.

The inductive helical stent is simulated at the initial crimped and expanded state. At crimped state, the stent is at the martensitic phase which has a lower electrical resistivity. When the stent is heated wirelessly, the stent expands and transforms into austenite. In a previous study [24], the crimped stent has a length of 21 mm and an

Figure 2. Simulation setup in HFSS.

Table 1. Properties of a nitinol.

Mass density (kg m^{-3})	6450
Relative electrical permittivity, ε_r	1
Relative magnetic permeability, μ_r	1.002
Electrical resistivity, ρ (Ω m)	8.2 x 10^{-7} (Austenite) 7.6 x 10^{-7} (Martensite)

external diameter of 2.2 mm. After wireless expansion, the stent diameter increases to 4.5 mm but decreases in stent length to 18 mm. In this simulation, the number of turns of the coil is 10 with each turn comprises 16 stent struts or 8 crowns in both states.

The inductive helical stent can be considered an irregular solenoid. However, as the analytical method using equations to solve the values of L, Q, and R is more usual in DC application, the method is less applicable to a device that works in AC mode. In addition, the aforementioned parameters are highly frequency-dependent at high frequency for wireless applications. Therefore, FEA is used as an alternative approach to simulating the values in frequency domain. In HFSS, the values L, Q, and R can be extracted from the admittance-parameter or Y-parameter. The values are obtained as output variables using equations as follows [25].

$$L = 10^9 \times \frac{\text{Im}\left[1/Y_{11}\right]}{2\pi f} nH \qquad (6)$$

$$Q = abs\left|\frac{\text{Im}\left[1/Y_{11}\right]}{\text{Re}\left[1/Y_{11}\right]}\right| \qquad (7)$$

$$R = \frac{1}{\text{Re}\left[1/Y_{11}\right]} \Omega \qquad (8)$$

where Y_{11} is the Y-parameter that can be obtained in HFSS.

4. RESULTS AND DISCUSSION

In this work, the value of L, Q, and R are simulated for different states of the stent: initial crimped and expanded. The simulated results of L and Q and R are shown in Figure 3 and 4 respectively. When a parallel-plate capacitor is substituted as the capacitive component of the LC circuit, an active stent with a resonant frequency is formed. When the inductive helical stent expands, the inductance changes. As a result, the resonant frequency of the device (active stent) will be shifted.

By referring to Figure 3, the frequency range where the Q-factor is high assures the functionality of an inductive helical stent as an ideal inductor when operating at the device resonant frequency. From Figure 3, the Q-factor of the crimped inductive helical stent peaks at a frequency of 315 MHz. Assuming this frequency is chosen as the desired resonant frequency for a crimped inductive helical
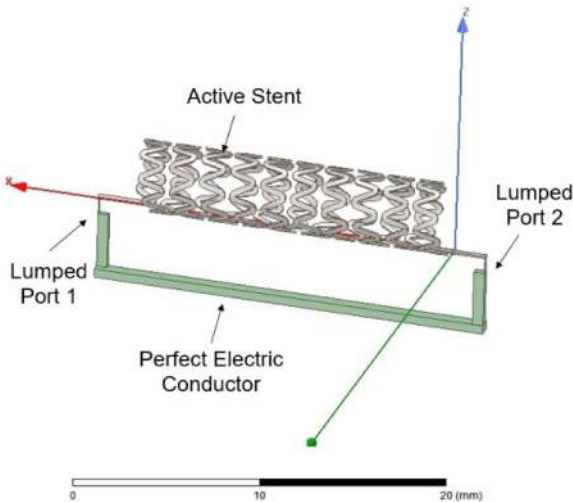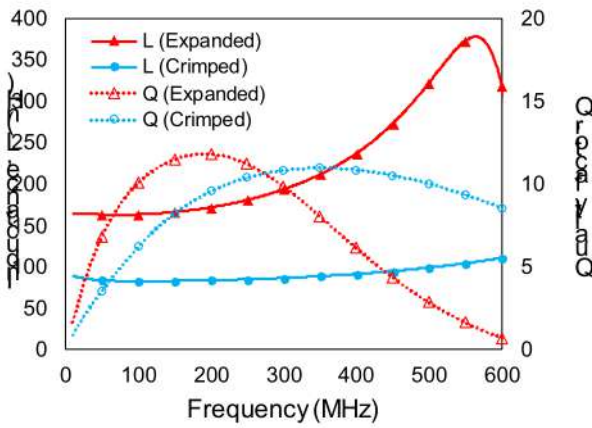
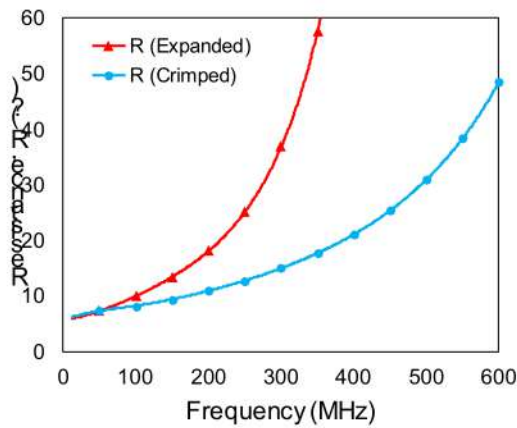Figure 3. Simulation result of L and Q in frequency domain.

Figure 4. Simulation result of R in frequency domain.

stent of 87.3 nH, the required capacitance value of the parallel-plate capacitor can be calculated as ~2.92 pF using Equation (1).

When the inductive helical stent expands, the inductance where the Q-factor peaks is around 170 nH. Using Equation (1) and C = 2.92 pF assuming a constant capacitance, the device resonant frequency at the expanded state will be around 226 MHz. This expanded state resonant frequency of 226 MHz lies within the region of high Q-factor which peaks at 190 MHz . Table 2 shows the tabulated data for the inductive helical stent at different states for comparison.

The values of series resistance in the frequency domain are depicted in Figure 4. The stent resistance increased from the initial 15.9 to 21.6 Ω when expanded wirelessly. This is due to the changes in the value of nitinol electrical resistivity at different states. The stent resistance is an important parameter to be considered because it contributes to AC joule heating during wireless stent expansion. However, the Q-factor is the ratio of inductive reactance to resistance. Therefore, a high value of inductance and a small value of resistance account for the high Q-factor of an inductive helical stent. When the Q-factor is increased, the wireless power transfer efficiency will be improved.

Table 2. Comparison between initial and expanded stent.

	Crimped	Expanded
Length (mm)	21	18
External diameter (mm)	2.2	4.5
Number of turns (N)	10	10
Resonant frequency, f_R (MHz)	315	226
Inductance (nH)	87.3	176
Quality factor	10.9	11.6
Series resistance (Ω)	15.9	21.6

5. CONCLUSION

A simulation for a novel SMA nitinol type active stent was performed via FEA. The FEA solution is used to assess the critical parameters that are important to wireless applications. The parameters are difficult to be calculated using the conventional analytical method. Using HFSS, the values of L, Q, and R were extracted from Y-parameter. The resonant frequencies of the device at different states lie within the high Q-factor region of the simulated results in this work. This shall provide easier access to evaluate the performance and feasibility of the device design.

REFERENCES

[1] Department of Statistics Malaysia, "Statistics on causes of death, Malaysia 2020," November 2020.
[2] World Health Organization, "The top 10 causes of death," December 2020.
[3] F. Alfonso and J. Cuesta, "The therapeutic dilemma of recurrent in-stent restenosis," *Circ.-Cardiovasc. Interv.,* vol. 11, pp. 1-4, 2018.
[4] A. Gaspardone and F. Versaci, "Coronary stenting and inflammation," *Am. J. Cardiol.,* vol. 96, no. 12, pp. 65-70, 2005.
[5] I. Akin, H. Schneider, H. Ince, S. Kische, T. Rehders, T. Chatterjee, and C. Nienaber, "Second-and third-generation drug-eluting coronary stents," *Herz,* vol. 36, no. 3, pp. 190-197, 2011.
[6] C. Stettler, S. Wandel, S. Allemann, A. Kastrati, M. C. Morice, A. Schömig, M. E. Pfisterer, G. W. Stone, M. B. Leon, and J. S. de Lezo, "Outcomes associated with drug-eluting and bare-metal stents: a

collaborative network meta-analysis," *Lancet,* vol. 370, no. 9591, pp. 937-948, 2007.

[7] A. Schömig, A. Dibra, S. Windecker, J. Mehilli, J. S. de Lezo, C. Kaiser, S.-J. Park, J.-J. Goy, J.-H. Lee, and E. Di Lorenzo, "A meta-analysis of 16 randomized trials of sirolimus-eluting stents versus paclitaxel-eluting stents in patients with coronary artery disease," *J. Am. Coll. Cardiol.,* vol. 50, no. 14, pp. 1373-1380, 2007.

[8] D. Yin, G. S. Mintz, L. Song, Z. Chen, T. Lee, A. J. Kirtane, M. A. Parikh, J. W. Moses, K. N. Fall, A. Jeremias, Z. A. Ali, R. A. Shlofmitz, and A. Maehara, "In-stent restenosis characteristics and repeat stenting underexpansion: insights from optical coherence tomography," *EuroIntervention,* vol. 16, no. 4, pp. e335-e343, 2020.

[9] A.-Y. Her and E.-S. Shin, "Current management of in-stent restenosis," *Korean Circ. J.,* vol. 48, no. 5, pp. 337-349, 2018.

[10] J. S. Bergstroem and D. Hayman, "An overview of mechanical properties and material modeling of polylactide (PLA) for medical applications," *Ann. Biomed. Eng.,* vol. 44, no. 2, pp. 330-340, 2016.

[11] Y. Zhu, K. Yang, R. Cheng, Y. Xiang, T. Yuan, Y. Cheng, B. Sarmento, and W. Cui, "The current status of biodegradable stent to treat benign luminal disease," *Mater. Today,* vol. 20, no. 9, pp. 516-529, 2017.

[12] P. W. Serruys, H. M. Garcia-Garcia, and Y. Onuma, "From metallic cages to transient bioresorbable scaffolds: change in paradigm of coronary revascularization in the upcoming decade?," *Eur. Heart J.,* vol. 33, no. 1, pp. 16-25, 2012.

[13] H. Jinnouchi, S. Torii, A. Sakamoto, F. D. Kolodgie, R. Virmani, and A. V. Finn, "Fully bioresorbable vascular scaffolds: lessons learned and future directions," *Nat. Rev. Cardiol.,* vol. 16, no. 5, pp. 286-304, 2019.

[14] X. Chen, B. Assadsangabi, Y. Hsiang, and K. Takahata, "Enabling angioplasty-ready "Smart" Stents to detect in-stent restenosis and occlusion," *Adv. Sci.,* vol. 5, no. 5, pp. 1700560, 2018.

[15] Y. Luo, X. Chen, M. Dahmardeh, and K. Takahata, "RF-powered stent with integrated circuit breaker for safeguarded wireless hyperthermia treatment," *J. Microelectromech. Syst.,* vol. 24, no. 5, pp. 1293-1302, 2015.

[16] Y. Yi, J. Chen, M. Selvaraj, Y. Hsiang, and K. Takahata, "Wireless hyperthermia stent system for restenosis treatment and testing with swine model," *IEEE Trans. Biomed. Eng.,* vol. 67, no. 4, pp. 1097-1104, 2019.

[17] C. J. Li, Y. F. Zheng, and L. C. Zhao, "Heating NiTi stent in magnetic fields and the thermal effect on smooth muscle cells," *Key Eng. Mater.,* vol. 288, pp. 579-582, 2005.

[18] X. Ji, J. Zheng, R. Yang, W. Kainz, and J. Chen, "Evaluations of the MRI RF-induced heating for helical stents under a 1.5 T MRI system," *IEEE Trans. Electromagn. Compat.,* vol. 61, no. 1, pp. 57-64, 2018.

[19] K. Takahata, Y. B. Gianchandani, and K. D. Wise, "Micromachined antenna stents and cuffs for monitoring intraluminal pressure and flow," *J. Microelectromech. Syst.,* vol. 15, no. 5, pp. 1289-1298, 2006.

[20] M. S. M. Ali, B. Bycraft, A. Bsoul, and K. Takahata, "Radio-controlled microactuator based on shape-memory-alloy spiral-coil inductor," *J. Microelectromech. Syst.,* vol. 22, no. 2, pp. 331-338, 2012.

[21] A. R. Mohammadi, M. S. M. Ali, D. Lappin, C. Schlosser, and K. Takahata, "Inductive antenna stent: design, fabrication and characterization," *J. Micromech. Microeng.,* vol. 23, no. 2, pp. 025015, 2013.

[22] H. H. Quick, H. Kuehl, G. Kaiser, S. Bosk, J. F. Debatin, and M. E. Ladd, "Inductively coupled stent antennas in MRI," *Magnetic Resonance in Medicine: An Official Journal of the International Society for Magnetic Resonance in Medicine,* vol. 48, no. 5, pp. 781-790, 2002.

[23] C.-H. Liu, S.-C. Chen, and H.-M. Hsiao, "A single-connector stent antenna for intravascular monitoring applications," *Sensors,* vol. 19, no. 21, pp. 4616, 2019.

[24] Y. X. Ang, F. A. M. Ghazali, and M. S. M. Ali, "Micromachined shape memory alloy active stent with wireless monitoring and re-expansion features," in *33rd IEEE Int. Conf. on Micro Electro Mechanical Systems (MEMS)*, Vancouver, Canada, 2020, pp. 396-399.

[25] C. Yang, F. Liu, T.-L. Ren, L.-T. Liu, G. Chen, X.-K. Guan, A. Wang, and H.-G. Feng, "Ferrite-integrated on-chip inductors for RF ICs," *IEEE Electron Device Lett.,* vol. 28, no. 7, pp. 652-655, 2007.